The Plant Cell, Vol. 20: 1231–1243, May 2008, www.plantcell.org © 2008 American Society of Plant Biologists

Dual Effects of miR156-Targeted *SPL* Genes and *CYP78A5/KLUH* on Plastochron Length and Organ Size in *Arabidopsis thaliana* [W] [OA]

Jia-Wei Wang, Rebecca Schwab,[1] Benjamin Czech,[1] Erica Mica,[2] and Detlef Weigel[3]

Department of Molecular Biology, Max Planck Institute for Developmental Biology, D-72076 Tübingen, Germany

Leaves of flowering plants are produced from the shoot apical meristem at regular intervals, with the time that elapses between the formation of two successive leaf primordia defining the plastochron. We have identified two genetic axes affecting plastochron length in *Arabidopsis thaliana*. One involves microRNA156 (miR156), which targets a series of *SQUAMOSA PROMOTER BINDING PROTEIN-LIKE* (*SPL*) genes. In situ hybridization studies and misexpression experiments demonstrate that miR156 is a quantitative, rather than spatial, modulator of *SPL* expression in leaf primordia and that *SPL* activity nonautonomously inhibits initiation of new leaves at the shoot apical meristem. The second axis is exemplified by a redundantly acting pair of cytochrome P450 genes, *CYP78A5*/*KLUH* and *CYP78A7*, which are likely orthologs of *PLASTOCHRON1* of rice (*Oryza sativa*). Inactivation of *CYP78A5*, which is expressed at the periphery of the shoot apical meristem, accelerates the leaf initiation rate, whereas *cyp78a5 cyp78a7* double mutants often die as embryos with supernumerary cotyledon primordia. The effects of both miR156-targeted *SPL* genes and *CYP78A5* on organ size are correlated with changes in plastochron length, suggesting a potential compensatory mechanism that links the rate at which leaves are produced to final leaf size.

INTRODUCTION

In the aerial part of flowering plants, all organs, including leaves, stems, and flowers, originate from a small population of stem cells. These cells are embedded in the shoot apical meristem, on the flanks of which new leaf and flower primordia are produced in a regular spatial and temporal pattern. The spatial pattern is known as phyllotaxis and can be, for example, spiral, alternating (distichous), or decussate (forming 180° angles). Most species show a single phyllotactic pattern, but in some cases, a plant can switch from one pattern to another in response to developmental or external cues. The temporal pattern is characterized by the time that elapses between the formation of primordia, called the plastochron, which is the inverse of the leaf initiation rate.

Classical surgical experiments have indicated that existing leaf primordia produce a diffusible substance that inhibits the formation of new primordia, with new primordia being formed at the position with a minimal inhibitor concentration (Snow, 1929). Recent analyses have suggested an alternative phyllotactic model that is based on positive effects of the growth hormone auxin (Reinhardt et al., 2000, 2003; Vernoux et al., 2000; Jönsson et al., 2006; Smith et al., 2006). According to this model, auxin is imported by the shoot apical meristem and redistributed primarily through the epidermal cell layer (L1), with existing primordia acting as auxin sinks. Additional auxin maxima can thus only form between existing primordia, once these are sufficiently spaced apart. New primordia are then initiated at these sites.

While there has been considerable progress in knowledge about how phyllotaxis is governed and what role auxin plays in this process, a coherent understanding of the regulation of plastochron length is lacking. Inactivation of several genes, including rice (*Oryza sativa*) *PLASTOCHRON1* (*PLA1*), maize (*Zea mays*) *TERMINAL EAR1* (*TE1*) and its rice ortholog *PLA2*, and *ALTERED MERISTEM PROGRAM1* (*AMP1*) in *Arabidopsis thaliana*, causes a shortening of the plastochron (Conway and Poethig, 1997; Itoh et al., 1998; Veit et al., 1998; Helliwell et al., 2001; Miyoshi et al., 2004; Kawakatsu et al., 2006). By contrast, *phytochrome b* (*phyb*) and *serrate* (*se*) mutants in *Arabidopsis* suffer from delayed initiation of new leaves (Reed et al., 1993; Clarke et al., 1999; Prigge and Wagner, 2001). All of these genes have pleiotropic effects, and the diverse nature of the encoded products, including a photoreceptor (*PHYB*), a cytochrome P450 enzyme (*PLA1*), and an RNA binding protein (*TE1*/*PLA2*), suggests a complex network for plastochron regulation in many species.

Several lines of evidence point to cytokinin as a regulator of leaf initiation. For example, *amp1* mutants contain elevated levels of cytokinin (Chaudhury et al., 1993), and overexpressing the *CYTOKININ OXIDASE1* (*CKX1*) gene increases plastochron length in *Arabidopsis* (Werner et al., 2003). Furthermore, maize plants lacking the *ABPHYL1* (*ABPH1*) gene have, like *amp1*

[1] Current address: Cold Spring Harbor Laboratory, Cold Spring Harbor, NY 11724.
[2] Current address: Department of Biomolecular Sciences and Biotechnology, University of Milan, 20133 Milan, Italy.
[3] Address correspondence to weigel@weigelworld.org.
The author responsible for distribution of materials integral to the findings presented in this article in accordance with the policy described in the Instructions for Authors (www.plantcell.org) is: Detlef Weigel (weigel@weigelworld.org).
[W] Online version contains Web-only data.
[OA] Open Access articles can be viewed online without a subscription.
www.plantcell.org/cgi/doi/10.1105/tpc.108.058180

mutants in *Arabidopsis*, a larger shoot apical meristem and altered phyllotaxy (Jackson and Hake, 1999; Nogué et al., 2000; Giulini et al., 2004). The *ABPH1* gene product belongs to a group of ARABIDOPSIS RESPONSE REGULATOR proteins, which are important modulators of the cytokinin response (Ferreira and Kieber, 2005). Related genes in *Arabidopsis* function directly downstream of the meristem regulator WUSCHEL (Leibfried et al., 2005). Nevertheless, how meristem size and cytokinin affect primordium formation or how this is regulated by crosstalk between auxin and cytokinin is unclear.

Here, we describe two genetic axes affecting plastochron length in *Arabidopsis*. One includes microRNA156 (miR156), which targets several *SQUAMOSA PROMOTER BINDING PROTEIN-LIKE* (*SPL*) transcription factor genes that are predominantly expressed at the shoot apex (Cardon et al., 1999; Rhoades et al., 2002; Schmid et al., 2003; Schwarz et al., 2008). By comparing endogenous expression domains of *SPL* genes with the results of misexpression studies, we demonstrate that miR156 limits plastochron length in developing leaf primordia. The effects of miR156/SPLs on leaf initiation rate appear to be independent of *CYP78A5/KLUH*, a likely ortholog of rice *PLA1* (Itoh et al., 1998; Zondlo and Irish, 1999; Miyoshi et al., 2004; Anastasiou et al., 2007). Interestingly, organ size and plastochron length are coordinately affected by both miR156/*SPL* and *CYP78A5*, suggesting either that there are common regulators of organ size and plastochron length or that these two developmental parameters reciprocally influence each other.

RESULTS

Role of miR156-Targeted *SPL* Genes in Determining Plastochron Length

Among previously described mutants with increased plastochron lengths is *se*-1 (Clarke et al., 1999), which is defective in the processing of several miRNAs, including miR156 (Lobbes et al., 2006; Yang et al., 2006; Laubinger et al., 2008; see Supplemental Figures 1A and 1B online). We found that leaf initiation was similarly affected in *ago1*-27 plants, which carry a weak mutant allele of *ARGONAUTE1* (*AGO*), the gene encoding the main slicer responsible for miRNA-directed transcript cleavage in *Arabidopsis* (Morel et al., 2002; Vaucheret et al., 2004; Baumberger and Baulcombe, 2005; see Supplemental Figure 1A online). Together, these observations indicate that an miRNA is limiting for the delay of the initiation of new leaf primordia. At least two lines of evidence suggest miR156 as the most promising candidate. First, overexpression of miR156 plants causes shortening of the plastochron (Schwab et al., 2005; see Supplemental Figure 1C online), a phenotype opposite to that of *se*-1 and *ago1*-27. Second, while *Pro35S:MIR156f se*-1 double mutants retained the serrated leaf phenotype typical of *se*-1 mutants, the plastochron defect caused by miR156 overexpression was suppressed in these plants (see Supplemental Figure 1C online).

In *Arabidopsis*, 11 of the 17 *SPL* genes are targeted by miR156 (Rhoades et al., 2002; Schwab et al., 2005; Gandikota et al., 2007). In microarray analyses, most miR156-targeted *SPLs* show similar patterns of RNA accumulation, with low levels in vegetative tissues and increased expression at the shoot apex upon flowering (Schmid et al., 2003; Schwab et al., 2005). However, the SPL proteins differ substantially in size. SPL3, SPL4, and SPL5 are much smaller than the other gene products, with the DNA binding domain making up most of the protein (Cardon et al., 1999). We identified several homozygous T-DNA insertion lines of miR156-targeted *SPLs*, including *spl2*, *spl3*, *spl9*, *spl10*, *spl11*, *spl13*, and *spl15* (Figure 1A; see Supplemental Figure 2A online). Similar to *spl3* mutants (Wu and Poethig, 2006), the other single-insertion mutants were phenotypically normal in terms of leaf initiation rate and flowering time (data not shown), indicating a high degree of functional redundancy.

Among the larger *SPL*s, two unlinked genes are particularly similar to each other, *SPL9* and *SPL15* (Cardon et al., 1999; Yang et al., 2008). We found that *spl9 spl15* double mutants had short plastochrons (Figure 1; see Supplemental Table 1 online), in agreement with a recent independent report (Schwarz et al., 2008). Although the phenotype was milder than that of the miR156 overexpressers, in which expression of eight additional *SPL* genes is strongly reduced (Schwab et al., 2005), this finding indicated an important redundant effect of *SPL9* and *SPL15* on plastochron length.

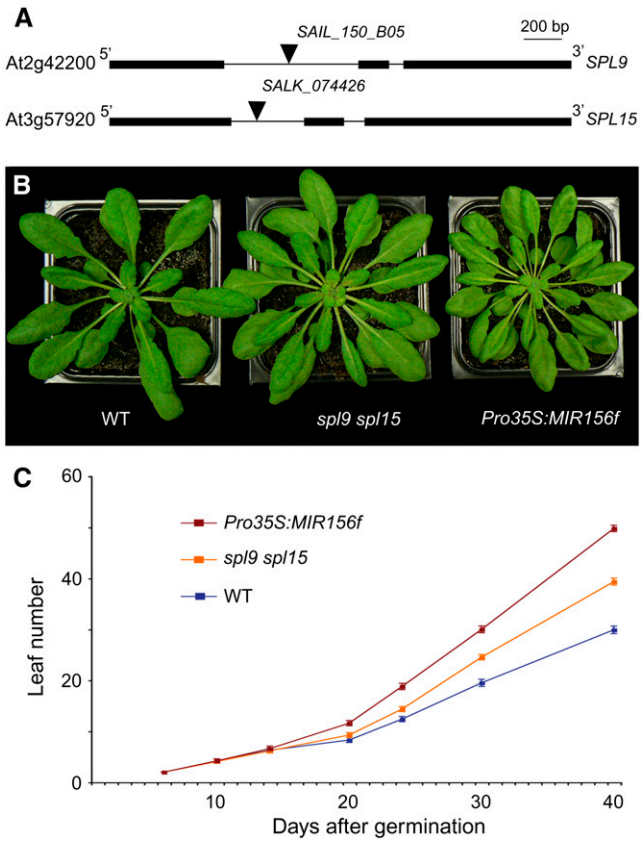

Figure 1. Modulation of Plastochron Length by *SPL* Genes.

(A) Diagram of *SPL9* and *SPL15* transcribed regions, with thin lines indicating introns. Arrowheads mark T-DNA insertion sites.
(B) Rosettes of 30-d-old short-day-grown plants.
(C) Appearance of visible leaves in wild-type, *Pro35S:MIR156f*, and *spl9 spl15* plants grown in short days ($n \geq 10$). Bars indicate SD.

Based on overexpression experiments, the *SPL3* gene has been implicated primarily in the regulation of flowering time and phase change (Cardon et al., 1997; Wu and Poethig, 2006). Unfortunately, knockout alleles for the other two small *SPL* genes, *SPL4* and *SPL5*, are not available, making it more difficult to test whether redundancy among the three small *SPL* genes masks their contribution to plastochron length. We therefore designed an artificial miRNA that targeted the mRNAs of both *SPL4* and *SPL5* (Schwab et al., 2006) (see Supplemental Figures 2B and 2C online) and introduced these into *spl3* mutants. These plants did not show obvious differences in plastochron length (data not shown), suggesting that the three small *SPL* genes likely play minor roles, if any, in the regulation of leaf initiation rate.

Effects of miR156 Misexpression

To understand how miR156 and its *SPL* targets modulate leaf initiation rate, we analyzed the effects of expressing miR156 in different domains of the shoot apex (Figure 2). We chose the promoter of *SHOOT MERISTEMLESS* (*STM*) for the shoot apical meristem (Kim et al., 2003), that of *FLOWERING LOCUS D* (*FD*) for the shoot apical meristem and leaf anlagen (Abe et al., 2005; Wigge et al., 2005), that of *LATERAL ORGAN BOUNDARIES* (*LOB*) for the periphery of the shoot apical meristem (Shuai et al., 2002), those of *AINTEGUMENTA* (*ANT*) and *ASYMMETRIC LEAVES1* (*AS1*) for young leaf primordia (Schoof et al., 2000; Eshed et al., 2001), that of the *SCARECROW* homolog *BLS* for late leaf primordia (Lifschitz et al., 2006), and that of the *SUCROSE-PROTON SYMPORTER2* (*SUC2*) for vascular tissue (Truernit and Sauer, 1995; Imlau et al., 1999). Specific activity of the promoters, as reported in the literature, was confirmed by promoter β-glucuronidase (GUS) fusions (see Supplemental Figure 3 online).

Because one can imagine that the rate of primordium initiation is largely determined by the number of cells available in the periphery of the meristem, we suspected that miR156 targets would limit plastochron length in the meristem itself. To our surprise, transgenic miR156 expression in the meristem proper (*ProFD:MIR156f* and *ProSTM:MIR156f*) did not affect leaf initiation rate (Figure 2; see Supplemental Table 1 online). Similar to *Pro35S:MIR156b* plants (Schwab et al., 2005), directing miR156 expression to the periphery of the shoot apical meristem with the *LOB* promoter did not change plastochron length either (Figure 2; see Supplemental Table 1 online). By contrast, expression of *MIR156f* under control of the leaf primordium–specific *ANT* and *AS1* promoters led to a similar plastochron phenotype to that seen in *Pro35S:MIR156f* plants. Thirty-day-old wild-type plants grown in short days had produced 20 leaves, whereas *ProANT:MIR156f* and *ProAS1:MIR156f* plants had produced 30 or half again as many leaves (Figure 2; see Supplemental Table 1 online). Finally, *ProBLS:MIR156f* and *ProSUC2:MIR156f* plants had an intermediate phenotype, indicating that misexpression of miR156 in older leaf primordia that already develop vasculature (or in the vasculature subtending the meristem proper) is less effective in altering plastochron length. Taken together, we conclude that miR156-targeted *SPL* genes contribute to nonautonomous effects of existing leaf primordia on the initiation of new leaf primordia at the shoot apical meristem.

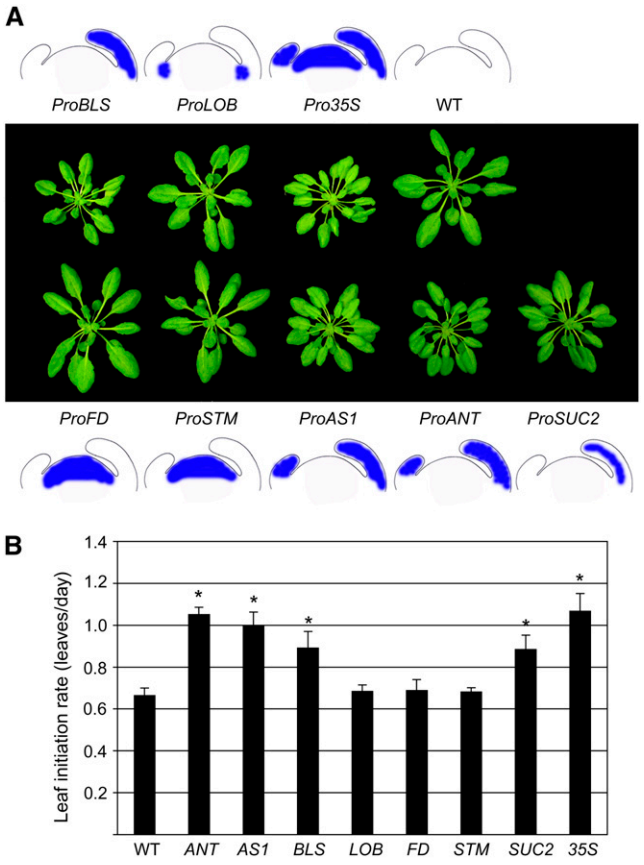

Figure 2. Effects of *MIR156f* Misexpression.

(A) Thirty-day-old short-day-grown transgenic plants expressing *MIR156f* from different promoters, with expression domains indicated by blue color in the accompanying illustrations of shoot apices (see Supplemental Figure 3 online for expression data).

(B) Leaf initiation rates of transgenic plants, calculated from short-day-grown T1 individuals ($n \geq 10$; see Supplemental Table 1 online). Bars indicate SD. Asterisks indicate a significant difference from the wild type (Student's *t* test with Bonferroni correction, $P < 0.04$).

Expression Pattern of *SPL9*

Consistent with other types of expression studies for *SPL3* (Cardon et al., 1997; Wu and Poethig, 2006), microarray analyses have shown that most miR156-targeted *SPL* genes have a similar RNA expression pattern, with the highest levels in the shoot apex and an increase in expression during the transition to flowering (Schmid et al., 2003; Schwab et al., 2005). We used in situ hybridization to analyze in more detail the expression pattern of *SPL9*. During the vegetative phase, *SPL9* mRNA was found in leaf anlagen and in developing leaf primordia (Figure 3A). As young leaves grew, *SPL9* expression became gradually restricted to vascular tissues. Importantly, we did not detect any *SPL9* transcripts in the central part of the meristem. In the inflorescence apex, the expression pattern of *SPL9* was similar to that in the vegetative shoot apex. *SPL9* mRNA was found only transiently in the youngest floral primordia (Figure 3B). In

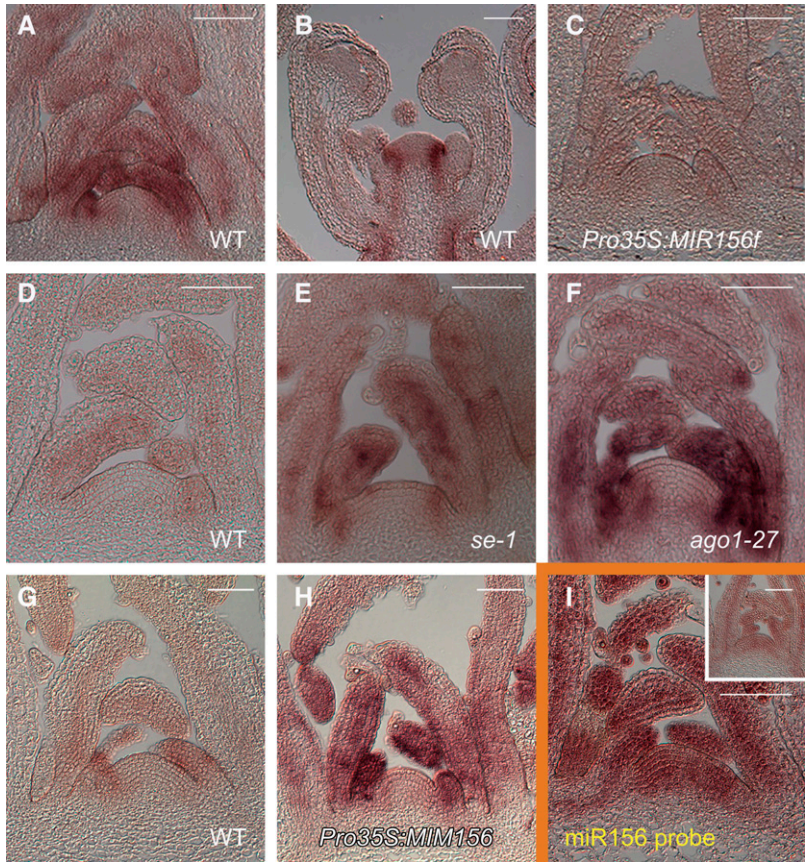

Figure 3. In Situ Hybridizations Showing Expression Patterns of *SPL9* and miR156.

(A) to **(H)** Expression of *SPL9*.
(A) and **(B)** Wild-type vegetative **(A)** and reproductive shoot apex **(B)**.
(C) *Pro35S:MIR156f* vegetative shoot apex.
(D) to **(F)** Wild-type, *se-1*, and *ago1-27* vegetative shoot apices. All three samples were stained for the same amount of time in the dark. The wild type was allowed to remain underdeveloped so that the stronger signals in the other two genotypes would not become saturated.
(G) and **(H)** Wild-type and *Pro35S:MIM156* vegetative apices. Both samples were stained for the same amount of time in the dark. The wild type was allowed to remain underdeveloped so that the stronger signal in the *Pro35S:MIM156* apex would not become saturated.
(I) Expression of miR156 in the wild type and *se*-1 (inset).
Shoot apices were dissected from 15-d-old plants grown in short days. Bars = 50 μm.

Pro35S:MIR156f plants, *SPL9* transcripts were strongly reduced (Figure 3C), confirming that miR156 can target *SPL9* mRNAs for degradation by miRNA-guided cleavage.

Since transgene-directed expression of miR156 in the meristem itself had little effect on plastochron length, one might conclude that this is the primary site of endogenous miR156 activity and that the main function of miR156 is to prevent accumulation of *SPL* transcripts in the meristem proper. We therefore analyzed *SPL9* expression in two mutants with reduced miR156 levels, *se*-1 and *ago1*-27. Compared with the wild type, *SPL9* RNA levels were substantially elevated in both mutants. However, the overall pattern of expression was similar to that seen in the wild type (Figures 3D to 3F). To exclude that this was an indirect effect of other miRNAs, we employed transgenic plants in which miR156 activity is specifically reduced by constitutive expression of a target mimic (Franco-Zorrilla et al., 2007). *SPL9* mRNA expression was changed in these *Pro35S:MIM156* plants in a similar manner as in *se*-1 and *ago1*-27 plants (Figures 3G and 3H).

The analysis of *SPL9* expression in mutants indicates that miR156 primarily affects *SPL9* expression in a quantitative, rather than spatial manner. That miR156 is not an important regulator of the domain of *SPL9* expression was also supported by a direct analysis of miR156 expression by in situ hybridization, which revealed that miR156 accumulated to similar levels in both the shoot apical meristem proper and leaf primordia (Figure 3I). The specificity of the hybridization signal was confirmed using *se*-1 plants, in which the level of miR156 was greatly reduced (Figure 3I, inset).

In summary, the expression studies confirm that *SPL9*, and likely other *SPL* genes, either mediate or trigger nonautonomous effects of existing leaf primordia on the initiation of new leaf

primordia by the meristem proper and that the primary role of miR156 is to dampen overall levels of *SPL* RNA (and probably also protein; Gandikota et al., 2007) in leaf primordia, rather than shaping its spatial expression pattern.

Increased Plastochron Length in Response to Elevated SPL9 and SPL10 Activity

To determine whether *SPL* genes are not only required to prevent shortening of plastochron length but are also sufficient to increase plastochron length, we prepared forms of *SPL* genes that can no longer be targeted by miR156 according to known rules for effective miRNA targeting in plants (Schwab et al., 2005). We refer to these mutants as nontargeted or resistant *SPL*s (*rSPL*s) (Figure 4A).

Overexpression of *rSPL3* caused early flowering as reported (Wu and Poethig, 2006; Gandikota et al., 2007) but caused only a minor decrease in leaf initiation rate (see Supplemental Table 1 online), suggesting limited crosstalk between miR156 targets of the *SPL3/4/5* and *SPL9/15* groups.

It was difficult to recover *Pro35S:rSPL9* plants, suggesting that very high levels of SPL9 protein cause embryonic lethality. Plants that expressed *rSPL9* under the control of the native promoter had a very strong plastochron phenotype, with the leaf initiation rate reduced to one-third of that of the wild type (Figures 4B and 4C; see Supplemental Table 1 online). We observed a similar, but weaker, phenotype in a few plants expressing the nonmutated form of *SPL9*, in line with the hypothesis of a quantitative interaction between miR156 and its targets. We confirmed that *rSPL9* is insensitive to miR156 action by introducing the *Pro35S:MIR156f* transgene into these plants. The doubly transgenic plants were indistinguishable from *ProSPL9:rSPL9* plants (Figure 4B).

The results presented in the previous two sections had suggested that *SPL9* functions nonautonomously in existing leaf primordia to time the emergence of new primordia from the shoot apical meristem. To assess whether SPL9 can also act directly in the meristem, we misexpressed *rSPL9* from different promoters. Ectopic expression from the primordium-specific *ANT* and *AS1* promoters reduced the number of leaves to less than half of that of the wild type after 30 d in short-day conditions. A similar phenotype was observed in *ProFD:rSPL9* plants (Figure 4B; see Supplemental Table 1 online), in which *SPL9* was ectopically expressed in the shoot meristem. Misexpression of *rSPL10* had similar, though less dramatic, effects than *rSPL9* (see Supplemental Table 1 online), consistent with overlapping roles of *SPL9* and *SPL10*, which both belong to the group of large *SPL* genes.

In summary, elevated activity of *SPL* genes can increase plastochron length, indicating an instructive role of the miR156/SPL axis in timing the emergence of new leaf primordia.

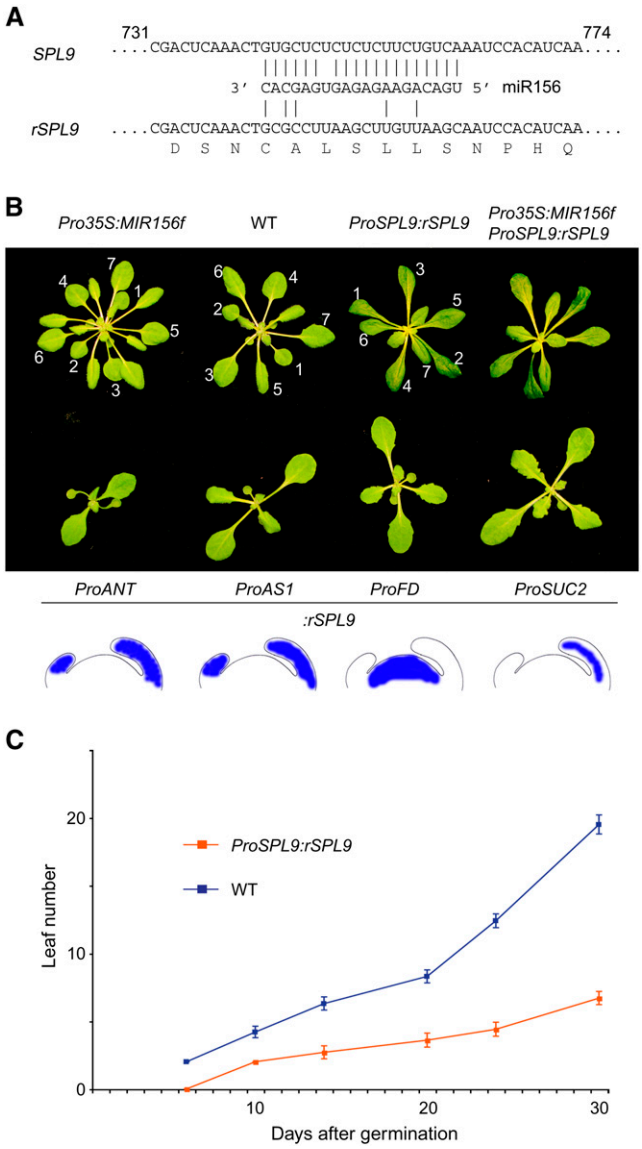

Figure 4. Effects of a miR156-Insensitive Form of *SPL9*.

(A) Diagram of the miR156 target sites of the wild-type and modified version of *SPL9*. Capital letters below indicate encoded amino acids.
(B) Forty-day-old (*ProSPL9:rSPL9* genotypes) and 20-d-old plants (all other genotypes) grown in short days. Misexpression of *rSPL9* with different promoters causes a similar delay in leaf initiation. Numbers indicate the order of leaves, with 1 referring to the oldest leaf. Note that there is no apparent disruption of normal phyllotaxis in plants with decreased or increased *SPL* activity.
(C) Appearance of visible leaves in short-day-grown plants ($n = 10$). Bars indicate SD.

Effects of *CYP78A5/KLUH* and *CYP78A7* on Plastochron Length

A short plastochron phenotype has also been described for rice plants with mutations in *PLA1*, which is likely an ortholog of *CYP78A5/KLUH* in *Arabidopsis*. Both genes are expressed at the periphery of the meristem proper and at the base of new leaf primordia (Zondlo and Irish, 1999; Miyoshi et al., 2004; Anastasiou et al., 2007). We found that *CYP78A5* loss-of-function mutants had shortened plastochrons in both long and short days. In

addition, the first flowers formed a few days earlier than in the wild type (Figures 5A to 5C; see Supplemental Table 2 online).

CYP78A5, located on chromosome 5, has a homolog on chromosome 1, *CYP78A7*. Unlike *cyp78a5*, the *cyp78a7* single mutant appeared phenotypically normal (see Supplemental Figure 4 online). To reveal functional redundancy between these two members, we crossed the *cyp78a5* and *cyp78a7* mutant lines. Because we did not readily identify double mutants in the F2 generation, we examined developing embryos in siliques of *cyp78a5*/*cyp78a5 cyp78a7*/+ plants. Little phenotypic change was observed among embryos in *cyp78a5*/*cyp78a5 cyp78a7*/+ siliques until the torpedo stage. From that stage on, almost a quarter of embryos did not increase much in size. The shoot apical meristem, however, continued to enlarge and became much bigger than the arrested cotyledons. The abnormal shoot apical meristem initiated supernumerary cotyledons (Figures 5D to 5G). The double mutants could sometimes survive, and we recovered a few *cyp78a5 cyp78a7* seedlings from a *cyp78a5*/*cyp78a5 cyp78a7*/+ parent (five double mutants among 87 progeny tested). These plants, which produced no seeds, were small with compacted rosette leaves and an increased leaf initiation rate. The seedlings had three or four cotyledons (see Supplemental Figure 4 online), similar to *amp1* mutants, which also have an embryonic phenotype reminiscent of *cyp78a5 cyp78a7* double mutants (Chaudhury et al., 1993; Conway and Poethig, 1997). In summary, these results indicate that *CYP78A5* and *CYP78A7* play redundant roles in regulating relative growth of the shoot apical meristem and the rest of the plant.

Genetic Interaction between miR156/*SPL* and *CYP78A5*

Our miR156 misexpression experiments indicated that miR156-targeted SPLs act predominantly in leaf primordia, while *CYP78A5* is expressed in the periphery of the shoot apical meristem (Zondlo and Irish, 1999). Nevertheless, given the phenotypic similarity of *Pro35S:MIR156f* and *cyp78a5* mutants, we wanted to test whether miR156/SPL and *CYP78A5* operate in the same genetic pathway. Since *SPL* genes encode transcription factors, we first assessed RNA expression levels. There was no significant change of *CYP78A5* transcript levels in either *Pro35S:MIR156f* or *ProSPL9:rSPL9* plants (Figure 6A). Similarly, *SPL9* levels were unaffected by *cyp78a5* (Figure 6A).

To further clarify the relationship between *CYP78A5* and the miR156/*SPL* pathway, we examined genetic interactions. The plastochron length of *ProSPL9:rSPL9 cyp78a5* plants was intermediate between that of the parental lines, which have opposite phenotypes, suggesting parallel effects of the two genetic systems. This was supported by the *Pro35S:MIR156f cyp78a5* combination, which had an even faster leaf initiation rate than either single mutant (Figure 6B).

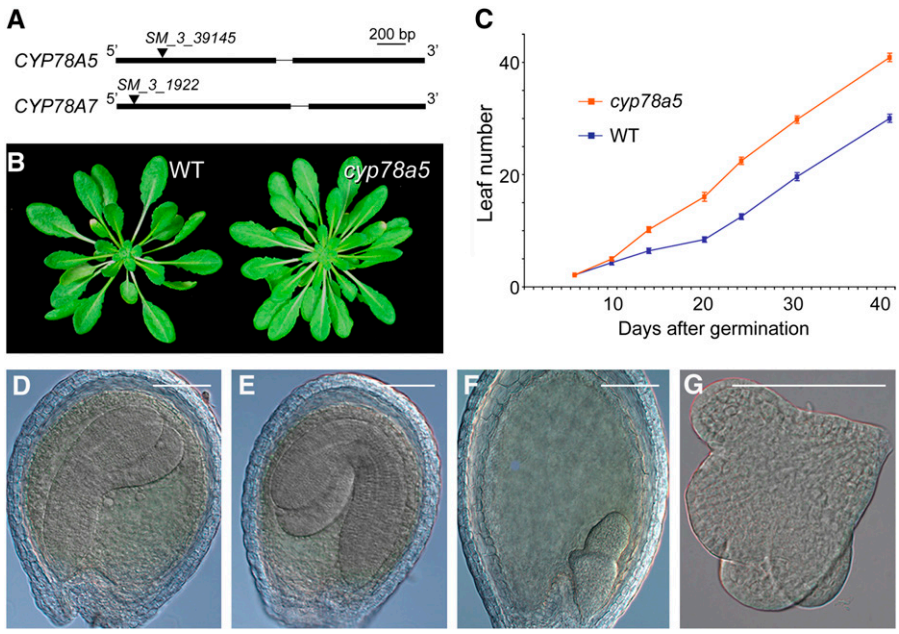

Figure 5. *cyp78a5* and *cyp78a7* Mutant Phenotypes.

(A) Diagram of *CYP78A5* and *CYP78A7* transcribed regions, with thin lines indicating introns. Arrowheads mark T-DNA insertion sites. The *cyp78a5* allele has also been described as *klu*-4 (Anastasiou et al., 2007).

(B) Rosettes of 30-d-old plants grown in short days.

(C) Appearance of visible leaves in short-day-grown plants ($n = 10$). Bars indicate SD.

(D) and **(E)** Wild-type embryos at bent-cotyledon stage **(D)** and at maturity **(E)**.

(F) and **(G)** *cyp78a5 cyp78a7* embryos at bent-cotyledon stage **(F)** and at maturity **(G)**. The latter was dissected from the seed coat. More than 10 siliques were examined, and representative embryos are shown. Note the enlarged shoot apical meristem in **(F)** and multiple cotyledons in **(G)**. Bars = 150 μm.

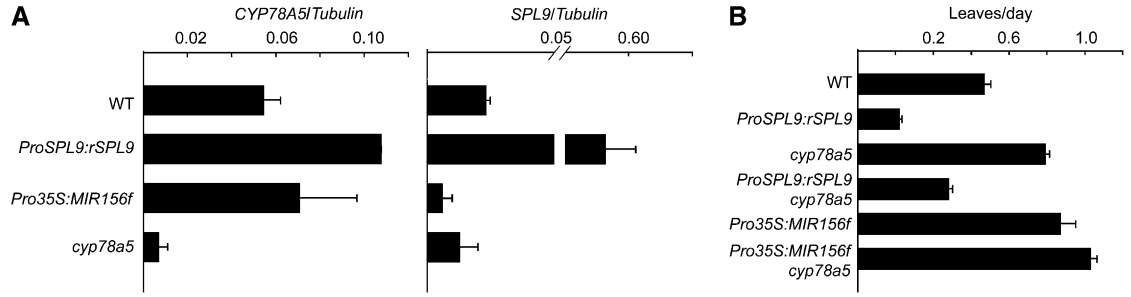

Figure 6. Genetic Interaction between miR156/*SPL* and *CYP78A5*.

(A) Expression of *CYP78A5* and *SPL9* in wild-type, mutant, and transgenic plants. Total RNA was extracted from 7-d-old long-day-grown plants and analyzed by real-time RT-PCR with three technical replicates. Expression was normalized relative to that of β-*TUBULIN2*. Two biological replicates were performed, both with similar results.

(B) Leaf initiation rate in wild-type, mutant, and transgenic plants, calculated from 10 short-day-grown individuals (see Supplemental Table 1 online). Bars indicate SD.

CYP78A5, also known as *KLUH*, has recently been implicated in growth regulation, with small leaves and floral organs in *cyp78a5* mutants because of prematurely arrested growth (Anastasiou et al., 2007), similar to what was shown for the apparent rice ortholog, *PLA1* (Itoh et al., 1998). We found that *Pro35S:MIR156f* plants, which have a similar plastochron phenotype to *cyp78a5* mutants, also exhibited smaller leaf size (Table 1; see Supplemental Figure 5 online). Similar effects on organ and cell size were observed in petals (see Supplemental Table 3 online). Thus, the effects of decreasing SPL activity on organ growth parallel the changes caused by inactivation of *PLA1* or *CYP78A5/KLUH* (Itoh et al., 1998; Anastasiou et al., 2007). Together, these observations support a close relationship between leaf growth and plastochron length.

Correlation between Plastochron Length, Cell Division Rate, and Meristem Size

From first principles, the leaf initiation rate could be affected either by the size of the meristem or by the rate of cell division in the meristem. Indeed, increased shoot apical meristem size in *clv1* mutants is paralleled by shortened plastochron length (Kwon et al., 2005). We therefore examined vegetative shoot apices by scanning electron microscopy. Meristem shape and phyllotaxis of *cyp78a5*, and *Pro35S:MIR156f* and *ProSPL9:rSPL9* plants were similar to those of the wild type, even though they had either shorter or longer plastochrons than the wild type, suggesting that the plastochron changes were not caused by defects in leaf positioning (Figures 7A to 7D). The two lines with shortened plastochrons, *cyp78a5* and *Pro35S:MIR156f*, had meristems of similar sizes to the wild type, while meristems were smaller in *ProSPL9:rSPL9* plants (Figure 7, Table 2).

Histone H4 is highly transcribed in G1-S cells and is a useful marker for cell division (Krizek, 1999; Gaudin et al., 2000). We performed in situ hybridization with different genotypes and counted the number of *Histone H4* positive cells per median longitudinal section (Table 2). We found that there were substantially fewer *Histone H4*–expressing cells in the *ProSPL9:rSPL9* shoot apical meristem (Figure 7F), suggesting that the increased plastochron length in *rSPL9* plants correlates with both fewer dividing cells and a smaller overall meristem. The picture was less clear for *cyp78a5* and *Pro35S:MIR156f* plants, which have normal-sized shoot apical meristems. There were more *Histone H4*–expressing cells in *cyp78a5* and *Pro35S:MIR156f* plants (Figure 7G), but the difference from the wild type was statistically significant only in *cyp78a5* (Table 2, Figures

Table 1. Leaf and Leaf Cell Sizes in Different Genotypes

	Wild Type	*cyp78a5*	*Pro35S:MIR156f*
First leaf length (mm)	8.20 ± 0.50	7.38 ± 0.23*	8.00 ± 0.21
First leaf width (mm)	7.58 ± 0.29	5.38 ± 0.23*	7.45 ± 0.33
Third leaf length (mm)	17.58 ± 0.36	12.54 ± 0.33*	13.13 ± 0.43*
Third leaf width (mm)	9.71 ± 0.58	8.04 ± 0.26*	9.21 ± 0.26
Largest leaf length (mm)	21.79 ± 0.81	17.42 ± 0.36*	17.38 ± 0.38*
Largest leaf width (mm)	12.79 ± 0.50	8.92 ± 0.42*	10.79 ± 0.45*
Cell size (μm^2)[a]	7446 ± 319	7436 ± 364	7314 ± 367

For each genotype, 12 20-d-old long-day-grown plants were scored. SD is given. Asterisks indicate significant difference from the wild type (Student's *t* test with Bonferroni correction, $P < 0.01$).

[a] Subepidermal palisade cells of the largest leaf were measured.

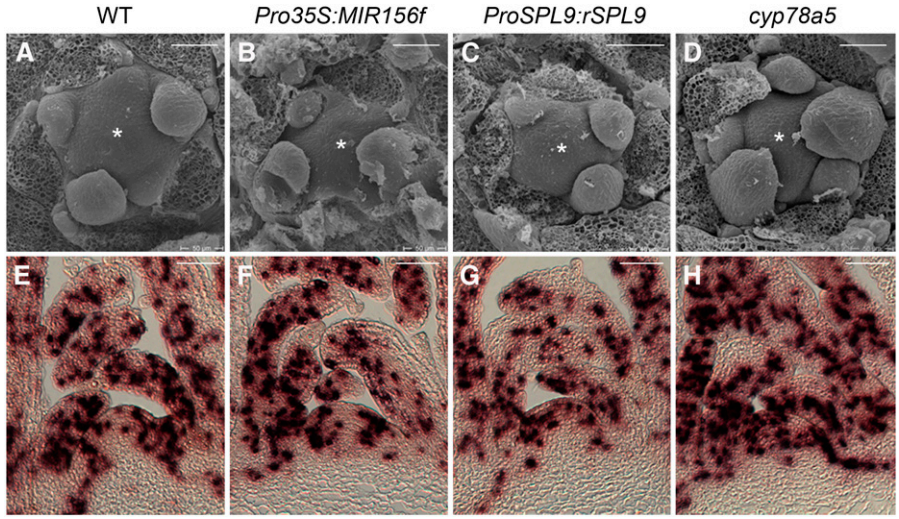

Figure 7. Morphology of Shoot Apical Meristem and Dividing Cells.

(A) to **(D)** Scanning electron micrographs of shoot apices from 30-d-old short-day-grown plants. At least 10 individuals were examined for each genotype, and representative images are shown.
(E) to **(H)** *Histone H4* expression in shoot apices of 15-d-old short-day-grown plants.
The *ProSPL9:rSPL9* plants were grown at a later time point, but the wild-type controls were similar as for the other two genotypes. Bars = 50 μm.

7E and 7G). Even so, together with the normal-sized shoot apical meristem, we conclude that more rapid cell division in the shoot apical meristems of both miR156-overexpressing plants and in *cyp78a5* mutants compensates for an increase in leaf initiation rate.

DISCUSSION

miR156 and its *SPL* targets have previously been shown to affect flowering time and phase change (Cardon et al., 1997; Schwab et al., 2005; Wu and Poethig, 2006). Here, we have described a critical role of miR156/*SPL* in regulating plastochron length. Although the miR156/SPL axis appears to act largely in parallel with *CYP78A5/KLUH*, the likely ortholog of rice *PLA1*, the two genetic systems have similar effects on both organ size and plastochron length, suggesting a regulatory link between these traits, which are important determinants of overall plant growth.

Regulation of *SPL* Expression by miR156

It had been initially proposed that plant miRNAs mostly control the spatial expression pattern of their targets (Juarez et al., 2004; Parizotto et al., 2004). However, in other cases, miRNAs seem to be important for both spatially confining target mRNAs and for dampening their levels (McConnell et al., 2001; Kidner and Martienssen, 2004; Sieber et al., 2007). In *se*-1 and *ago1*-27 mutants as well as *Pro35S:MIM156* plants, all of which have reduced miR156 activity, we observed a clear increase in the levels of the *SPL9* target mRNA but no obvious expansion of its expression domain. Thus, miR156 appears to be at the other end of possibilities for miRNA target interactions, with its main role being quantitative control of target mRNA levels, similar to what has been reported for miR169 and its targets in snapdragon (*Antirrhinum majus*) and petunia (*Petunia hybrida*; Cartolano et al., 2007). This conclusion is supported by a comparison of *SPL9* and miR156 expression patterns, which strongly overlap (Figure 3).

Nonautonomous Effects on Plastochron Length

Classic experiments have shown that removal of young leaf primordia accelerates the rate of leaf initiation at the shoot apex (Snow, 1929). Based on this finding, it has been proposed that

Table 2. Shoot Apical Meristem Characteristics of Different Genotypes Grown for 30 d in Short Photoperiods

Genotype	Leaves/Day	Width (μm)	Height (μm)	H4 Positive Cells[a]
Wild type	0.66 ± 0.03	125.2 ± 0.8	40.3 ± 0.8	16.0 ± 0.81
cyp78a5	0.98 ± 0.05*	125.8 ± 0.9	39.6 ± 0.8	19.1 ± 1.3*
Pro35S:MIR156f	1.07 ± 0.08*	125.7 ± 1.1	38.8 ± 0.8	17.1 ± 0.89
ProSPL9:rSPL9	0.23 ± 0.01*	96.9 ± 2.1*	32.2 ± 1.1*	11.4 ± 0.78*

$n = 10$ for all genotypes. SD is given. Asterisks indicate significant difference from the wild type (Student's *t* test with Bonferroni correction, $P < 0.015$).
[a] Number of *Histone H4* positive cells per longitudinal section.

young leaf primordia synthesize an inhibitory, mobile factor that acts in the meristem proper. Two lines of evidence indicate that the miR156/SPL axis fits the tenets of this hypothesis. First, overexpression of miR156 in leaves or leaf primordia shortens plastochron length, whereas increased SPL activity in the leaf primordium has an opposite effect. Second, at least one of the *SPL* genes, *SPL9*, is predominantly expressed in leaf primordia.

Auxin is required for the initiation of leaf primordia, and blocking auxin transport or signaling inhibits primordium formation (Reinhardt et al., 2000, 2003; Benkova et al., 2003). Since existing leaf primordia, as auxin sinks, have an important effect on the generation of new auxin maxima, which then direct the initiation of new primordia, it is formally possible that SPLs affect plastochron length by modulating auxin accumulation or sensitivity. A similar formal possibility is that SPL proteins themselves are the mobile signal, which would be consistent with our observation that overexpressing *SPL*s in either leaf primordia or the meristem proper had similar effects on plastochron length. The latter observations also conform to a model in which a secondary inhibitor is directly regulated by SPLs. Some of these alternatives could be resolved by identifying direct targets of SPL transcription factors.

Several other genes have similar effects on plastochron length to those of the miR156/SPL axis. Mutations in both *TE1* and in its rice ortholog *PLA2* cause shortened plastochrons (Itoh et al., 1998; Veit et al., 1998; Miyoshi et al., 2004). These genes encode RNA binding proteins related to yeast MEI2, a master regulator of meiosis (Ohno and Mattaj, 1999). Both are preferentially expressed in young leaf primordia, and they could potentially act in a pathway dependent on miR156 and its *SPL* targets, which are conserved in monocotyledonous plants (Xie et al., 2006; Chuck et al., 2007). Consistent with this hypothesis is the finding that *PLA2* appears to function independently of *PLA1* in rice (Kawakatsu et al., 2006), similar to the relationship between miR156/SPLs and *CYP78A5* in *Arabidopsis*. Unfortunately, it is unclear whether *TE1*/*PLA2* homologs fulfill related roles in *Arabidopsis*, especially since the most similar genes, *TEL1* and *TEL2*, are expressed in the shoot apical meristem only, different from *TE1* and *PLA2* (Anderson et al., 2004).

In contrast with the case for *PLA2*, a clear candidate for a *PLA1* ortholog exists in *Arabidopsis*, *CYP78A5/KLUH*, which delays the initiation of new leaves, just like *PLA1* (Itoh et al., 1998; Miyoshi et al., 2004; this work). The phenotype of embryos that lack activity of both *CYP78A5* and its most similar *Arabidopsis* homolog, *CYP78A7*, is reminiscent of *amp1* mutants (Chaudhury et al., 1993; Conway and Poethig, 1997). The *cyp78a* double mutant phenotype appears to be stronger than that of *amp1* mutants, being often embryonic lethal and always causing several cotyledons to develop in surviving seedlings. *AMP1* encodes an enzyme with unknown substrate (Helliwell et al., 2001; Vidaurre et al., 2007), and it remains to be seen whether the CYP78A5/7 and AMP1 proteins operate in the same metabolic pathway.

Plastochron Length and Shoot Apical Meristem Size

Several reports have suggested that plastochron length and shoot apical meristem size are inversely correlated. Increased meristem size and shortened plastochron characterize *clv1* mutants (Kwon et al., 2005), while the opposite is true of plants that overexpress *CKX* genes (Werner et al., 2003). A longer plastochron is also seen in plants with mutations in multiple cytokinin receptor genes (Riefler et al., 2006). These observations are consistent with our finding that *ProSPL9:rSPL9* plants have both a reduced meristem and increased plastochron length.

There is, however, no simple correlation between shoot apical meristem size and plastochron length, as neither miR156-overexpressing plants nor *cyp78a5* mutants have strongly enlarged shoot apical meristems, despite a substantial shortening of plastochron length. In these plants, it appears that the increase in plastochron length is mostly due to increased cell division rates, which is also the case in several rice mutants, including *pla1* and *pla2* (Itoh et al., 1998; Ikeda et al., 2005; Kawakatsu et al., 2006). A direct link between cell division and plastochron length has been made with plants that overexpress *Cyclin D2*, which leads to faster leaf initiation correlated with higher cell division rates. At least early on, size and organization of the shoot apical meristem are normal in these plants (Cockcroft et al., 2000; Boucheron et al., 2005). However, while cell division can under certain circumstances be limiting for shortening plastochron length, slowing down cell division with a dominant-negative version of CDC2a, a cyclin-dependent kinase that interacts with Cyclin D2, did not affect leaf initiation rate, apparently because increased cell size compensated for lower cell numbers (Hemerly et al., 1995).

Plastochron Length and Phase Change

Another defect of plants with reduced SPL activity due to miR156 overexpression is a delay in phase change, with the opposite effect caused by constitutive overexpression of an miRNA-insensitive version of *SPL3* (Wu and Poethig, 2006). An even stronger phenotype is seen in *ProSPL9:rSPL9* plants, in which the juvenile phase is lost (this work). Clonal analyses with maize have indicated that vegetative phase change is not conferred by the shoot apical meristem, but rather that phase identity is determined autonomously in each leaf primordium (Orkwiszewski and Poethig, 2000). Our results are consistent with this observation, as *SPL9* is normally expressed in leaf primordia, and increasing *SPL9* levels in leaf primordia by expression from the *ANT* promoter is sufficient to accelerate phase change.

A similar correlation between reduced plastochron length and delayed phase change is seen in rice *pla1* and *pla2* mutants (Itoh et al., 1998; Kawakatsu et al., 2006). A net outcome of this would be that phase change is more normal in these mutants when measured in absolute time. However, there does not seem to be an inevitable link between plastochron length and phase change. For example, *Teopod* mutants in maize suffer from delayed phase change, but leaf initiation rates are normal (Poethig, 1988). Conversely, inactivation of the *TAS3* pathway causes an acceleration of phase change. However, leaf initiation rates are not altered in *RNA-dependent RNA polymerase6*, *dicer-like4*, or *zippy/ago7* mutants (J.-W. Wang and D. Weigel, unpublished results), all of which are affected in *TAS3*-dependent phase change (Hunter et al., 2003, 2006; Xie et al., 2005; Adenot et al.,

2006; Fahlgren et al., 2006; Garcia et al., 2006). As with meristem size, the relationship between phase change and plastochron length is complex.

A Compensatory Mechanism Linking Plastochron Length and Organ Size?

A final phenotype that is shared between several mutants is the reduced size of leaves and floral organs (Itoh et al., 1998; Veit et al., 1998; Kawakatsu et al., 2006; Anastasiou et al., 2007; this work). An increase in plastochron length, at least during inflorescence development, has also been suggested for the *big brother* mutant, which has enlarged organs as well (Disch et al., 2006). Similar to how coordinated changes in plastochron length and phase change would maintain the absolute timing of phase change, an effect of organ size on plastochron length or vice versa would lead to overall biomass changes being kept to a minimum. There is precedence for a related phenomenon during leaf growth, namely the compensation of changes in cell size by total cell number (Horiguchi et al., 2006). Alternatively, rather than organ size and plastochron length reciprocally affecting each other, one can envision that coordinated behavior of the two traits is due to a common regulator. Nevertheless, the connection between organ size and plastochron length is not static. For example, manipulating leaf size by altering activity of the *STRUBBELIG-RECEPTOR FAMILY4* gene (Eyüboglu et al., 2007) does not have the same effects on plastochron length as altering miR156/SPL activity (K. Schneitz, personal communication).

In summary, we have described how and where the miR156/SPL axis affects plastochron length and organ size and found that it acts largely independently of *CYP78A5/KLUH*, despite similar mutant phenotypes. Apart from the nature of the leaf-derived signal that affects plastochron length, an important challenge for future studies is the question of how ubiquitous coordinated changes in plastochron length and leaf size are.

METHODS

Oligonucleotide primers used in this work are given in Supplemental Table 4 online.

Plant Material

Arabidopsis thaliana plants, ecotype Columbia (Col-0), were grown at 23°C in long days (16 h light/8 h dark) or short days (8 h light/16 h dark). Individual *spl* and *cyp78a* T-DNA insertion lines (Tissier et al., 1999; Sessions et al., 2002; Alonso et al., 2003) were obtained from the European Arabidopsis Stock Centre (http://Arabidopsis.info). The *cyp78a5* allele has also been described as *klu*-4 (Anastasiou et al., 2007). miR156 target mimic expressing *Pro35S:MIM156* plants have been described (Franco-Zorrilla et al., 2007).

Transgenic Plants

For promoter fusions, *AS1* and *BLS* promoters were amplified by PCR with *AS1:LhG4* or *BLS:LhG4* plasmid DNA as templates. All other promoters and *SPL* genes were amplified by PCR with genomic DNA from Col-0 as template, using Turbo Hotstart *Pfu* DNA polymerase (Stratagene). *rSPL9* was made by two rounds of mutagenic PCR using Turbo Hot-start Pfu DNA polymerase (Stratagene). An artificial miRNA construct against SPL4 and *SPL*5 was generated as described (Schwab et al., 2006). The binary constructs were delivered into *Agrobacterium tumefaciens* strain GV3101 (pMP90RK) by the freeze-thaw method (Weigel and Glazebrook, 2002). *Arabidopsis* plants were transformed using the flower-dip method (Clough and Bent, 1998). Transgenic seedlings were selected with 50 μg/mL kanamycin on plates or 0.1% glufosinate (BASTA) on soil. At least 50 T1 seedlings were analyzed for each construct.

GUS Staining and Histology

One-week-old seedlings were fixed in 90% acetone for 20 min on ice. GUS staining was performed as described (Blázquez et al., 1997). Stained tissue was embedded, sectioned, and mounted in Clarion Mounting Medium (Sigma-Aldrich). Developing embryos were dissected from siliques and mounted in a mixture of chloralhydrate/glycerol/water (8:1:2) and photographed using differential interference contrast optics.

Expression Analysis

Total RNA was extracted from 1-week-old seedlings or vegetative shoot apices with the Plant RNeasy Mini kit (Qiagen). One microgram of total RNA was treated with DNase I and used for cDNA synthesis with oligo(dT) primer and Superscript reverse transcriptase (Invitrogen). Quantitative RT-PCR was performed with SYBR-Green PCR Mastermix (Invitrogen), and amplification was real-time monitored on an Opticon continuous fluorescence detection system (MJR). For small RNA gel blots, a mixed DNA/locked nucleic acid (LNA; Exiqon; Wahlestedt et al., 2000) oligonucleotide probe (gtg^{m}CtcAct^{m}CtcTgt^{m}Ca, where uppercase letters indicate LNA bases and lowercase letters DNA bases) was used.

In Situ Hybridization

SPL9 and *Histone H4* cDNAs were PCR amplified and cloned into pGEM-T easy (Promega). Digoxigenin-labeled sense and antisense probes were synthesized with T7 or SP6 RNA polymerase (Roche). For the miR156 probe, LNA oligonucleotides were end labeled with the DIG oligonucleotide 3′-end labeling kit (Roche). Shoot apices from 20-d-old short-day-grown plants were dissected and fixed in formalin/acetic acid/ethanol (1:1:18). Paraffin-embedded material was sectioned to 8 μm thickness. Hybridization and detection were performed as previously described (Palatnik et al., 2003).

Scanning Electron Microscopy and Shoot Apical Meristem and Organ Size Measurement

Vegetative shoot apices of 30-d-old short-day-grown plants were dissected, fixed in methanol, washed twice with 100% ethanol, critical point dried, and mounted. After gold coating, at least 10 apices per genotype were examined on a Hitachi S800 electron microscope. For size measurements, apices were embedded in paraffin and sectioned. The width and height of the meristem were scored for each section. To measure cell size, the leaves or petals were dissected, incubated in 80% ethanol for 2 h, mounted on slides with a drop of chloralhydrate/glycerol/water (8:1:2), and photographed using differential interference contrast optics. Cell size was calculated using AxioVision software (Zeiss).

Leaf Initiation Rate Measurement

The number of visible leaves (~1 mm in width) was recorded daily. Average leaf initiation rate was calculated by dividing total leaf number by days after germination.

Accession Numbers

Arabidopsis Genome Initiative gene identifiers are as follows: *SPL2* (At5g43270), *SPL3* (At2g33810), *SPL4* (At1g53160), *SPL5* (At3g15270), *SPL9* (At2g42200), *SPL10* (At1g27370), *SPL11* (At1g27360), *SPL13* (At5g50670), *SPL15* (At3g57920), *CYP78A5* (At1g13710), *CYP78A7* (At5g09970), *LOB* (At5g63090), *SUC2* (At1g22710), *FD* (At4g35900), *BLS* (At3g49950), *STM* (At1g62360), *ANT* (At4g37750), *AS1* (At2g37630), β-*TUBULIN-2* (At5g62690), and *Histone H4* (At5g59690).

Supplemental Data

The following materials are available in the online version of this article.

Supplemental Figure 1. miRNA Dependence of Plastochron Length.

Supplemental Figure 2. T-DNA Insertion Mutants and amiRNA Targeting *SPL4*/*5.*

Supplemental Figure 3. Activity of Promoter Fusions.

Supplemental Figure 4. Phenotype of the *cyp78a5 cyp78a7* Double Mutant.

Supplemental Figure 5. Leaf and Cell Size in Wild-Type, Mutant, and Transgenic Plants.

Supplemental Table 1. Leaf Initiation Rates of Different Genotypes.

Supplemental Table 2. Flowering Time of *cyp78a5* Mutants.

Supplemental Table 3. Petal and Petal Cell Size of Different Genotypes.

Supplemental Table 4. Oligonucleotide Primer Sequences.

ACKNOWLEDGMENTS

We thank the European Arabidopsis Stock Centre for seeds, Yuval Eshed for the *AS1* and *BLS* promoter constructs, Marco Todesco for *Pro35S:MIM156* plants, Jürgen Berger for scanning electron microscopy, Kay Schneitz for communicating unpublished data, and members of Team MiRNA for discussion. This work was supported by an EMBO Long-Term Fellowship to J.-W.W. (ALTF 274-2006), by a DFG-SFB 446 grant, and by European Community FP6 IPs SIROCCO (Contract LSHG-CT-2006-037900) and AGRON-OMICS (Contract LSHG-CT-2006-037704).

Received January 17, 2008; revised April 8, 2008; accepted May 1, 2008; published May 20, 2008.

REFERENCES

Abe, M., Kobayashi, Y., Yamamoto, S., Daimon, Y., Yamaguchi, A., Ikeda, Y., Ichinoki, H., Notaguchi, M., Goto, K., and Araki, T. (2005). FD, a bZIP protein mediating signals from the floral pathway integrator FT at the shoot apex. Science **309:** 1052–1056.

Adenot, X., Elmayan, T., Lauressergues, D., Boutet, S., Bouche, N., Gasciolli, V., and Vaucheret, H. (2006). DRB4-dependent *TAS3* trans-acting siRNAs control leaf morphology through AGO7. Curr. Biol. **16:** 927–932.

Alonso, J.M., et al. (2003). Genome-wide insertional mutagenesis of *Arabidopsis thaliana.* Science **301:** 653–657.

Anastasiou, E., Kenz, S., Gerstung, M., MacLean, D., Timmer, J., Fleck, C., and Lenhard, M. (2007). Control of plant organ size by *KLUH*/*CYP78A5*-dependent intercellular signaling. Dev. Cell **13:** 843–856.

Anderson, G.H., Alvarez, N.D.G., Gilman, C., Jeffares, D.C., Trainor, V.C.W., Hanson, M.R., and Veit, B. (2004). Diversification of genes encoding Mei2-Like RNA binding proteins in plants. Plant Mol. Biol. **54:** 653–670.

Baumberger, N., and Baulcombe, D.C. (2005). *Arabidopsis* ARGONAUTE1 is an RNA Slicer that selectively recruits microRNAs and short interfering RNAs. Proc. Natl. Acad. Sci. USA **102:** 11928–11933.

Benkova, E., Michniewicz, M., Sauer, M., Teichmann, T., Seifertova, D., Jürgens, G., and Friml, J. (2003). Local, efflux-dependent auxin gradients as a common module for plant organ formation. Cell **115:** 591–602.

Blázquez, M.A., Soowal, L., Lee, I., and Weigel, D. (1997). *LEAFY* expression and flower initiation in *Arabidopsis.* Development **124:** 3835–3844.

Boucheron, E., Healy, J.H., Bajon, C., Sauvanet, A., Rembur, J., Noin, M., Sekine, M., Riou-Khamlichi, C., Murray, J.A., Van Onckelen, H., and Chriqui, D. (2005). Ectopic expression of *Arabidopsis CYCD2* and *CYCD3* in tobacco has distinct effects on the structural organization of the shoot apical meristem. J. Exp. Bot. **56:** 123–134.

Cardon, G., Hohmann, S., Klein, J., Nettesheim, K., Saedler, H., and Huijser, P. (1999). Molecular characterisation of the *Arabidopsis* SBP-box genes. Gene **237:** 91–104.

Cardon, G., Hohmann, S., Nettesheim, K., Saedler, H., and Huijser, P. (1997). Functional analysis of the *Arabidopsis thaliana* SBP-box gene *SPL3*: A novel gene involved in the floral transition. Plant J. **12:** 367–377.

Cartolano, M., Castillo, R., Efremova, N., Kuckenberg, M., Zethof, J., Gerats, T., Schwarz-Sommer, Z., and Vandenbussche, M. (2007). A conserved microRNA module exerts homeotic control over *Petunia hybrida* and *Antirrhinum majus* floral organ identity. Nat. Genet. **39:** 901–905.

Chaudhury, A.M., Letham, S., Craig, S., and Dennis, E.S. (1993). *amp1* — A mutant with high cytokinin levels and altered embryonic pattern, faster vegetative growth, constitutive photomorphogenesis and precocious flowering. Plant J. **4:** 907–916.

Chuck, G., Cigan, A.M., Saeteurn, K., and Hake, S. (2007). The heterochronic maize mutant *Corngrass1* results from overexpression of a tandem microRNA. Nat. Genet. **39:** 544–549.

Clarke, J.H., Tack, D., Findlay, K., Van Montagu, M., and Van Lijsebettens, M. (1999). The *SERRATE* locus controls the formation of the early juvenile leaves and phase length in *Arabidopsis.* Plant J. **20:** 493–501.

Clough, S.J., and Bent, A.F. (1998). Floral dip: A simplified method for *Agrobacterium*-mediated transformation of *Arabidopsis thaliana.* Plant J. **16:** 735–743.

Cockcroft, C.E., den Boer, B.G.W., Healy, J.M.S., and Murray, J.A.H. (2000). Cyclin D control of growth rate in plants. Nature **405:** 575–579.

Conway, L.J., and Poethig, R.S. (1997). Mutations of *Arabidopsis thaliana* that transform leaves into cotyledons. Proc. Natl. Acad. Sci. USA **94:** 10209–10214.

Disch, S., Anastasiou, E., Sharma, V.K., Laux, T., Fletcher, J.C., and Lenhard, M. (2006). The E3 ubiquitin ligase BIG BROTHER controls *Arabidopsis* organ size in a dosage-dependent manner. Curr. Biol. **16:** 272–279.

Eshed, Y., Baum, S.F., Perea, J.V., and Bowman, J.L. (2001). Establishment of polarity in lateral organs of plants. Curr. Biol. **11:** 1251–1260.

Eyüboglu, B., Pfister, K., Haberer, G., Chevalier, D., Fuchs, A., Mayer, K.F.X., and Schneitz, K. (2007). Molecular characterisation of the *STRUBBELIG-RECEPTOR FAMILY* of genes encoding putative leucine-rich repeat receptor-like kinases in *Arabidopsis thaliana.* BMC Plant Biol. **7:** 16.

Fahlgren, N., Montgomery, T.A., Howell, M.D., Allen, E., Dvorak, S.K., Alexander, A.L., and Carrington, J.C. (2006). Regulation of *AUXIN RESPONSE FACTOR3* by *TAS3* ta-siRNA affects developmental timing and patterning in *Arabidopsis.* Curr. Biol. **16:** 939–944.

Ferreira, F.J., and Kieber, J.J. (2005). Cytokinin signaling. Curr. Opin. Plant Biol. **8:** 518–525.

Franco-Zorrilla, J.M., Valli, A., Todesco, M., Mateos, I., Puga, M.I., Rubio-Somoza, I., Leyva, A., Weigel, D., García, J.A., and Paz-Ares, J. (2007). Target mimicry provides a new mechanism for regulation of microRNA activity. Nat. Genet. **39:** 1033–1037.

Gandikota, M., Birkenbihl, R.P., Hohmann, S., Cardon, G.H., Saedler, H., and Huijser, P. (2007). The miRNA156/157 recognition element in the 3′ UTR of the Arabidopsis SBP box gene *SPL3* prevents early flowering by translational inhibition in seedlings. Plant J. **49:** 683–693.

Garcia, D., Collier, S.A., Byrne, M.E., and Martienssen, R.A. (2006). Specification of leaf polarity in *Arabidopsis* via the *trans*-acting siRNA pathway. Curr. Biol. **16:** 933–938.

Gaudin, V., Lunness, P.A., Fobert, P.R., Towers, M., Riou-Khamlichi, C., Murray, J.A., Coen, E., and Doonan, J.H. (2000). The expression of D-cyclin genes defines distinct developmental zones in snapdragon apical meristems and is locally regulated by the *CYCLOIDEA* gene. Plant Physiol. **122:** 1137–1148.

Giulini, A., Wang, J., and Jackson, D. (2004). Control of phyllotaxy by the cytokinin-inducible response regulator homologue *ABPHYL1.* Nature **430:** 1031–1034.

Helliwell, C.A., Chin-Atkins, A.N., Wilson, I.W., Chapple, R., Dennis, E.S., and Chaudhury, A. (2001). The Arabidopsis *AMP1* gene encodes a putative glutamate carboxypeptidase. Plant Cell **13:** 2115–2125.

Hemerly, A., Engler, J., Bergounioux, C., Van Montagu, M., Engler, G., Inzé, D., and Ferreira, P. (1995). Dominant negative mutants of the Cdc2 kinase uncouple cell division from iterative plant development. EMBO J. **14:** 3925–3936.

Horiguchi, G., Ferjani, A., Fujikura, U., and Tsukaya, H. (2006). Coordination of cell proliferation and cell expansion in the control of leaf size in *Arabidopsis thaliana.* J. Plant Res. **119:** 37–42.

Hunter, C., Sun, H., and Poethig, R.S. (2003). The Arabidopsis heterochronic gene *ZIPPY* is an *ARGONAUTE* family member. Curr. Biol. **13:** 1734–1739.

Hunter, C., Willmann, M.R., Wu, G., Yoshikawa, M., de la Luz Gutiérrez-Nava, M., and Poethig, S.R. (2006). Trans-acting siRNA-mediated repression of ETTIN and ARF4 regulates heteroblasty in *Arabidopsis.* Development **133:** 2973–2981.

Ikeda, K., Nagasawa, N., and Nagato, Y. (2005). *ABERRANT PANICLE ORGANIZATION 1* temporally regulates meristem identity in rice. Dev. Biol. **282:** 349–360.

Imlau, A., Truernit, E., and Sauer, N. (1999). Cell-to-cell and long-distance trafficking of the green fluorescent protein in the phloem and symplastic unloading of the protein into sink tissues. Plant Cell **11:** 309–322.

Itoh, J.I., Hasegawa, A., Kitano, H., and Nagato, Y. (1998). A recessive heterochronic mutation, *plastochron1*, shortens the plastochron and elongates the vegetative phase in rice. Plant Cell **10:** 1511–1522.

Jackson, D., and Hake, S. (1999). Control of phyllotaxy in maize by the *abphyl1* gene. Development **126:** 315–323.

Jönsson, H., Heisler, M.G., Shapiro, B.E., Meyerowitz, E.M., and Mjolsness, E. (2006). An auxin-driven polarized transport model for phyllotaxis. Proc. Natl. Acad. Sci. USA **103:** 1633–1638.

Juarez, M.T., Kui, J.S., Thomas, J., Heller, B.A., and Timmermans, M.C. (2004). microRNA-mediated repression of *rolled leaf1* specifies maize leaf polarity. Nature **428:** 84–88.

Kawakatsu, T., Itoh, J.-I., Miyoshi, K., Kurata, N., Alvarez, N., Veit, B., and Nagato, Y. (2006). *PLASTOCHRON2* regulates leaf initiation and maturation in rice. Plant Cell **18:** 612–625.

Kidner, C.A., and Martienssen, R.A. (2004). Spatially restricted microRNA directs leaf polarity through ARGONAUTE1. Nature **428:** 81–84.

Kim, J.Y., Yuan, Z., and Jackson, D. (2003). Developmental regulation and significance of KNOX protein trafficking in *Arabidopsis.* Development **130:** 4351–4362.

Krizek, B.A. (1999). Ectopic expression of *AINTEGUMENTA* in *Arabidopsis* plants results in increased growth of floral organs. Dev. Genet. **25:** 224–236.

Kwon, C.S., Chen, C., and Wagner, D. (2005). WUSCHEL is a primary target for transcriptional regulation by SPLAYED in dynamic control of stem cell fate in *Arabidopsis.* Genes Dev. **19:** 992–1003.

Laubinger, S., Sachsenberg, T., Zeller, G., Busch, W., Lohmann, J.U., Rätsch, G., and Weigel, D. (2008). Dual roles of the nuclear cap binding complex and SERRATE in pre-mRNA splicing and microRNA processing in *Arabidopsis thaliana.* Proc. Natl. Acad. Sci. USA, in press.

Leibfried, A., To, J.P., Busch, W., Stehling, S., Kehle, A., Demar, M., Kieber, J.J., and Lohmann, J.U. (2005). WUSCHEL controls meristem function by direct regulation of cytokinin-inducible response regulators. Nature **438:** 1172–1175.

Lifschitz, E., Eviatar, T., Rozman, A., Shalit, A., Goldshmidt, A., Amsellem, Z., Alvarez, J.P., and Eshed, Y. (2006). The tomato *FT* ortholog triggers systemic signals that regulate growth and flowering and substitute for diverse environmental stimuli. Proc. Natl. Acad. Sci. USA **103:** 6398–6403.

Lobbes, D., Rallapalli, G., Schmidt, D.D., Martin, C., and Clarke, J. (2006). SERRATE: A new player on the plant microRNA scene. EMBO Rep. **7:** 1052–1058.

McConnell, J.R., Emery, J., Eshed, Y., Bao, N., Bowman, J., and Barton, M.K. (2001). Role of *PHABULOSA* and *PHAVOLUTA* in determining radial patterning in shoots. Nature **411:** 709–713.

Miyoshi, K., Ahn, B.-O., Kawakatsu, T., Ito, Y., Itoh, J.-I., Nagato, Y., and Kurata, N. (2004). *PLASTOCHRON1*, a timekeeper of leaf initiation in rice, encodes cytochrome P450. Proc. Natl. Acad. Sci. USA **101:** 875–880.

Morel, J.-B., Godon, C., Mourrain, P., Beclin, C., Boutet, S., Feuerbach, F., Proux, F., and Vaucheret, H. (2002). Fertile hypomorphic *ARGONAUTE* (*ago1*) mutants impaired in post-transcriptional gene silencing and virus resistance. Plant Cell **14:** 629–639.

Nogué, F., Grandjean, O., Craig, S., Dennis, E., and Chaudhury, A. (2000). Higher levels of cell proliferation rate and cyclin *CycD3* expression in the *Arabidopsis amp1* mutant. Plant Growth Regul. **32:** 275–283.

Ohno, M., and Mattaj, I.W. (1999). Meiosis: MeiRNA hits the spot. Curr. Biol. **9:** R66–R69.

Orkwiszewski, J.A.J., and Poethig, R.S. (2000). Phase identity of the maize leaf is determined after leaf initiation. Proc. Natl. Acad. Sci. USA **97:** 10631–10636.

Palatnik, J.F., Allen, E., Wu, X., Schommer, C., Schwab, R., Carrington, J.C., and Weigel, D. (2003). Control of leaf morphogenesis by microRNAs. Nature **425:** 257–263.

Parizotto, E.A., Dunoyer, P., Rahm, N., Himber, C., and Voinnet, O. (2004). In vivo investigation of the transcription, processing, endonucleolytic activity, and functional relevance of the spatial distribution of a plant miRNA. Genes Dev. **18:** 2237–2242.

Poethig, R.S. (1988). Heterochronic mutations affecting shoot development in maize. Genetics **119:** 959–973.

Prigge, M.J., and Wagner, D.R. (2001). The Arabidopsis *SERRATE* gene encodes a zinc-finger protein required for normal shoot development. Plant Cell **13:** 1263–1280.

Reed, J.W., Nagpal, P., Poole, D.S., Furuya, M., and Chory, J. (1993). Mutations in the gene for the red/far-red light receptor phytochrome B alter cell elongation and physiological responses throughout Arabidopsis development. Plant Cell **5:** 147–157.

Reinhardt, D., Mandel, T., and Kuhlemeier, C. (2000). Auxin regulates the initiation and radial position of plant lateral organs. Plant Cell **12:** 507–518.

Reinhardt, D., Pesce, E.-R., Stieger, P., Mandel, T., Baltensperger, K., Bennett, M., Traas, J., Friml, J., and Kuhlemeier, C. (2003). Regulation of phyllotaxis by polar auxin transport. Nature **426:** 255–260.

Rhoades, M.W., Reinhart, B.J., Lim, L.P., Burge, C.B., Bartel, B., and Bartel, D.P. (2002). Prediction of plant microRNA targets. Cell **110:** 513–520.

Riefler, M., Novak, O., Strnad, M., and Schmülling, T. (2006). *Arabidopsis* cytokinin receptor mutants reveal functions in shoot growth, leaf senescence, seed size, germination, root development, and cytokinin metabolism. Plant Cell **18:** 40–54.

Schmid, M., Uhlenhaut, N.H., Godard, F., Demar, M., Bressan, R., Weigel, D., and Lohmann, J.U. (2003). Dissection of floral induction pathways using global expression analysis. Development **130:** 6001–6012.

Schoof, H., Lenhard, M., Haecker, A., Mayer, K.F.X., Jürgens, G., and Laux, T. (2000). The stem cell population of *Arabidopsis* shoot meristems in maintained by a regulatory loop between the *CLAVATA* and *WUSCHEL* genes. Cell **100:** 635–644.

Schwab, R., Ossowski, S., Riester, M., Warthmann, N., and Weigel, D. (2006). Highly specific gene silencing by artificial microRNAs in *Arabidopsis.* Plant Cell **18:** 1121–1133.

Schwab, R., Palatnik, J.F., Riester, M., Schommer, C., Schmid, M., and Weigel, D. (2005). Specific effects of microRNAs on the plant transcriptome. Dev. Cell **8:** 517–527.

Schwarz, S., Grande, A.V., Bujdoso, N., Saedler, H., and Huijser, P. (2008). The microRNA regulated SBP-box genes SPL9 and SPL15 control shoot maturation in Arabidopsis. Plant Mol. Biol. **67:** 183–195.

Sessions, A., et al. (2002). A high-throughput Arabidopsis reverse genetics system. Plant Cell **14:** 2985–2994.

Shuai, B., Reynaga-Pena, C.G., and Springer, P.S. (2002). The *LATERAL ORGAN BOUNDARIES* gene defines a novel, plant-specific gene family. Plant Physiol. **129:** 747–761.

Sieber, P., Wellmer, F., Gheyselinck, J., Riechmann, J.L., and Meyerowitz, E.M. (2007). Redundancy and specialization among plant microRNAs: role of the *MIR164* family in developmental robustness. Development **134:** 1051–1060.

Smith, R.S., Guyomarc'h, S., Mandel, T., Reinhardt, D., Kuhlemeier, C., and Prusinkiewicz, P. (2006). A plausible model of phyllotaxis. Proc. Natl. Acad. Sci. USA **103:** 1301–1306.

Snow, R. (1929). The young leaf as the inhibiting organ. New Phytol. **28:** 345–348.

Tissier, A.F., Marillonnet, S., Klimyuk, V., Patel, K., Torres, M.A., Murphy, G., and Jones, J.D.G. (1999). Multiple independent defective suppressor-mutator transposon Insertions in Arabidopsis: A tool for functional genomics. Plant Cell **11:** 1841–1852.

Truernit, E., and Sauer, N. (1995). The promoter of the *Arabidopsis thaliana SUC2* sucrose-H^+ symporter gene directs expression of β-glucuronidase to the phloem: Evidence for phloem loading and unloading by SUC2. Planta **196:** 564–570.

Vaucheret, H., Vazquez, F., Crété, P., and Bartel, D.P. (2004). The action of *ARGONAUTE1* in the miRNA pathway and its regulation by the miRNA pathway are crucial for plant development. Genes Dev. **18:** 1187–1197.

Veit, B., Briggs, S.P., Schmidt, R.J., Yanofsky, M.F., and Hake, S. (1998). Regulation of leaf initiation by the terminal ear 1 gene of maize. Nature **393:** 166–168.

Vernoux, T., Kronenberger, J., Grandjean, O., Laufs, P., and Traas, J. (2000). PIN-FORMED 1 regulates cell fate at the periphery of the shoot apical meristem. Development **127:** 5157–5165.

Vidaurre, D.P., Ploense, S., Krogan, N.T., and Berleth, T. (2007). *AMP1* and *MP* antagonistically regulate embryo and meristem development in *Arabidopsis.* Development **134:** 2561–2567.

Wahlestedt, C., et al. (2000). Potent and nontoxic antisense oligonucleotides containing locked nucleic acids. Proc. Natl. Acad. Sci. USA **97:** 5633–5638.

Weigel, D., and Glazebrook, J. (2002). Arabidopsis: A Laboratory Manual. (Cold Spring Harbor, NY: Cold Spring Harbor Laboratory Press).

Werner, T., Motyka, V., Laucou, V., Smets, R., Van Onckelen, H., and Schmülling, T. (2003). Cytokinin-deficient transgenic Arabidopsis plants show multiple developmental alterations indicating opposite functions of cytokinins in the regulation of shoot and root meristem activity. Plant Cell **15:** 2532–2550.

Wigge, P.A., Kim, M.C., Jaeger, K.E., Busch, W., Schmid, M., Lohmann, J.U., and Weigel, D. (2005). Integration of spatial and temporal information during floral induction in *Arabidopsis.* Science **309:** 1056–1059.

Wu, G., and Poethig, R.S. (2006). Temporal regulation of shoot development in *Arabidopsis thaliana* by miR156 and its target SPL3. Development **133:** 3539–3547.

Xie, K., Wu, C., and Xiong, L. (2006). Genomic organization, differential expression, and interaction of SQUAMOSA promoter-binding-like transcription factors and microRNA156 in rice. Plant Physiol. **142:** 280–293.

Xie, Z., Allen, E., Wilken, A., and Carrington, J.C. (2005). DICER-LIKE 4 functions in trans-acting small interfering RNA biogenesis and vegetative phase change in *Arabidopsis thaliana.* Proc. Natl. Acad. Sci. USA **102:** 12984–12989.

Yang, L., Liu, Z., Lu, F., Dong, A., and Huang, H. (2006). SERRATE is a novel nuclear regulator in primary microRNA processing in *Arabidopsis.* Plant J. **47:** 841–850.

Yang, Z., Wang, X., Gu, S., Hu, Z., Xu, H., and Xu, C. (2008). Comparative study of SBP-box gene family in *Arabidopsis* and rice. Gene **407:** 1–11.

Zondlo, S.C., and Irish, V.F. (1999). *CYP78A5* encodes a cytochrome P450 that marks the shoot apical meristem boundary in *Arabidopsis.* Plant J. **19:** 259–268.